Ultrasonic internal defect detection in cheese

Vincent Leemans*, Marie-France Destain

Gembloux Agricultural University – Unité de mécanique et construction

Passage des Déportés, 2 – B 5030 Gembloux, Belgium

Abstract

Different ultrasonic signals and detection techniques were used and compared to detect internal foreign bodies present in semi-soft cheeses. The signals were a pulse or a chirp and the detection was carried out by using either correlation with a reference signal or a wavelet decomposition. The principle of the detection consisted in measuring the time of flight of the transmitted signals and of the echoes, the latter in the absence of foreign body should be the double of the former. The presence of a foreign object affected this pattern in several ways. In order to assess the method, a small plastic cylindrical object of 3 mm in diameter was introduced in one half of the cheese and was tested for detection, the second half being used as reference for the control cheese. The results showed that the two signals and the two detection methods were able to localise the transmitted signals and the echo from the opposite face of the cheese under all circumstances. For the foreign body detection, the correlation method gave superior results, in term of signal to noise ratio as well as in term of error rate, while the two signals gave similar results. The analysis of the mean and standard deviation of the signal to noise ratio of the object echo showed that some samples presented peak values close to those due to the noise. Nevertheless, the object was detected in 90% of the tests. There was no significant effect of temperature on the detection technique.

Keywords : ultrasound; defect detection; chirp; wavelet; cheese.

* Corresponding author. Tel.: +32 81 62 21 61; fax +32 81 62 21 67.

Email address : leemans.v@fsagx.ac.be

1. Introduction

The presence of foreign bodies in food is a major concern in food industry and is one of the main reasons leading to prosecutions. In this paper, the term 'foreign body' refers to an unwanted object buried in the food product (e.g. metal, glass, plastic, …). Graves et al. (1998) detailed different methods to find foreign objects in food products. Magnetic systems and X-rays have gained widespread use on a commercial scale. The former are cheap and accurate but limited to the detection of metallic elements, while the latter are useful for finding both metallic and non-metallic dense foreign bodies inside a food product and its packaging. However, X-rays present limitation because of the short time available for scanning, limiting the resolution and the density contrast (McFarlane et al., 2001).

Ultrasound is a high-frequency sound that has the capability of penetrating opaque materials non-destructively. It is often used for the characterization of food materials despite encountering practical problems. Coupland (2004) mentioned that many foods have a strong attenuation that can make the measurement difficult and that multiple variables may affect the ultrasonic properties. However, the technique is used successfully to measure different properties such as the moisture content of food products or the solid fat content (Mc Clement, 1995, Povey and Mason, 1998 and Coupland, 2004), the rheological properties of cheese (Lee et al., 1992) or the maturity of cheese samples (Benedito et al., 2000). Few authors have reported the use of ultrasound to detect foreign bodies in food. Hæggström and Luukkala (2001) showed how to identify foreign bodies in food with a soft consistency such as margarine, marmalade or soft cheese. They immersed the tested sample in a water basin also containing the ultrasound probe. The signal was a 350 V pulse and the echo was pre-amplified and digitized. The echo signals of a sample without foreign body were subtracted from those of the studied sample including a foreign body. The result was treated amongst others by filtering and by computing Fourier transform. All the objects were detected, based on a signal-to-noise ratio. Their position was deduced from the time of flight of the echo. Cho and

Irudayarai 2003 tested non contact ultrasound to detect defects and internal objects in cheddar cheese block (thickness, 25 mm) and in skinless poultry breast. These authors showed that the relative attenuation could be used to detect the objects and that absolute values are needed to recognize the differences between internal disorder and foreign bodies. Zhao et al. (2006) used backscattered signals for detecting foreign bodies adhering to the inner walls of a bottle but this problem is in essence different, since time gating (measuring and comparing the time of flight of different signals) was not usable, which is not the case for the technique presented in this paper.

In the present work our objective was to analyse the potential of ultrasound to detect foreign bodies buried in food products. A piece of semi-soft cheese, tested whole, was used as a model food system. The research focused on the selection of input signals and mathematical treatment of the response.

2. Materials and methods

The classical method to assess foreign bodies or cracks in materials by using ultrasonic measurement is to apply a signal on one face of the object and to observe the transmitted signal on the other face and / or the echo on the face where it was applied. Preliminary studies showed that in pulse-echo mode, the amplitude of the signal obtained for whole cheese, including its crusts, gave a ratio relative to the pulse amplitude of 40 dB in the transmitted signal and a value around 60 dB in the echo. The echo of a small object was less intense than this. In order to limit the hardware cost, the probe emitting the signal was the same as the one that acquired the echo, which means that the input signal and the echo were both applied to the acquisition board. Under this circumstance, the signal to noise ratio of the echo is in general unfavourable. Hence this research focuses on a way to enhance the detection of the signals.

2.1. Hardware

The device was composed of two piezoelectric transducers (Panametrics A314S) in contact

with the cheese and placed facing each other (Fig. 1). The natural frequency of the sensors was 1 MHz and its bandwidth was 0.35 MHz. Input signals were applied to one of the sensors at regular intervals of 0.1 seconds (using a board ref. 5421, National Instruments, Austin, Texas, U.S.A., hereafter referenced as NI). The echo was measured by this transducer while the transmitted signal was acquired by the sensor opposite. An acquisition board digitised both signals (NI board ref. 5122). The sampling rates were conditioned by the subsequent treatment and are given in section 2.7. A controlled force of 4 N was applied to the upper probe.

All signal were treated on-line using LabView (NI), while the evaluations and their properties were evaluated off-line using GNU Octave (John W. Eaton, University of Wisconsin, Department of Chemical Engineering, Madison, WI, U.S.A.).

2.2. Cheese

The cheese studied in this work was produced by Maredsous (Belgium). It is an enzyme coagulated, surface ripened, semi-soft cheese of Trappist type, according to the classification given in Gunasekaran and Ak (2003). Its thickness was 55 mm. It was tested whole, with the crust. Six samples were considered.

The foreign body (noted FB) was a plastic cylindrical object having a diameter of 3 mm (a pen core). It was inserted half way into the cheese as shown in Fig. 1. This plastic object was selected not only because detectors for metallic objects are already available commercially, but because the closeness in the value of the acoustic impedance of plastic and cheese pose greater challenges. Further, its small size (around two wave lengths) makes it difficult to detect. The other half of the cheese, where no object was buried, served as a control.

The elastic properties of the cheese vary with temperature. As the acoustic impedance and the acoustic power coefficient (Hæggström and Luukkala, 2001) vary accordingly, the evaluation was carried out in temperature steps of one degree Celsius with the cheese warmed up to 17 °C after it was taken out of a fridge maintained at 3-4 °C up. The temperature was measured at the

centre of the cheese, as shown in Fig. 1.

At each temperature, ten replicate reading were taken on the part containing the FB as well as the control. The measurements were carried out on the two parts sequentially.

2.3. Input signals

Two different input signals were studied. The first one, l_p, was a classical 12 Volt, 0.2 μsec pulse and the second one was a "chirp", l_c, given by :

$$l_c = 6\left[1-\cos\left(\frac{2\pi t}{T}\right)\right]\sin\left(\omega t+\frac{\pi B t^2}{T}\right) \quad (1)$$

where t is the time, T is the period of the chirp, ω is the angular frequency and is B a time-independent parameter. The settings of these parameters were based on the natural frequency response of the transducers, giving $\omega = \pi\times10^6$ Hz and $B = 10^6$ Hz, and on the time of flight (TOF), giving T = 0.0002 sec. Figure 2 gives a graphical representation of this signal. Compared to the pulse, this input signal has the advantage of containing more energy without requiring a higher amplitude.

2.4. Output signal detection

The transmitted signal had a lower amplitude. Nevertheless, preliminary studies showed that the shape of the signal was only slightly affected by its transfer through the cheese, regardless of whether it was in the transmission or echo. Two methods were then compared to extract the output signal (hereafter denoted *x*) from the noise and hence to detect the signal. In the first case, the position of the signal was determined by cross-correlation between the signal *x* and a reference signal (denoted *y*). This reference was either a parametric model of the output signal for the pulse input or the chirp itself. In the second method, the output signal was decomposed into wavelet coefficients and the most significant ones were studied. This latter method was only applied to the pulse signal.

121 2.4.1. Detection by using cross-correlation

122 Figure 3 shows the response of a pulse excitation, with the probes placed one against the other,
123 without the sample (the grey curve). It can be seen that the response consists in an asymmetric
124 bell shape envelope and a sinusoidal signal carrier. The output signal *y* could thus be modelled
125 by the following expression :

$$y = c \cdot \sin(2\pi \nu t + \phi) \cdot \chi^2(at + b, n) \quad (2)$$

126 where *t* is the time elapsed since the emission of the pulse; ν is the frequency of the signal; ϕ is
127 the phase; χ^2 is a chi-square function with *n* degrees of freedom (controlling the asymmetry of
128 the envelope curve); *a*, *b* and *c* are constants determining respectively the "bell's" width, the
129 time lag and the maximum amplitude. The latter five parameters (ϕ, *n*, *a*, *b* and *c)* were fitted
130 to the signal using gradient descent which is also shown in Fig. 3 (thin black curve). A model
131 was preferred to the signal itself because this latter included echoes which resulted in multiple
132 correlation peaks.

133 When a sample was placed between the probes, the amplitudes of the signal were reduced and
134 the delay between the emission of the pulse and the reception of the signal grew, but the shape
135 remained unaffected, as evident in Fig. 4-a. The signal could thus be found by cross-correlation
136 (Preumont, 1990). To perform this operation, the function in Eq. 2 was digitised and each
137 signal acquired was compared with it. While applying the chirps, the theoretical input signal
138 given by Eq. 1 was also digitised and directly used as reference signal.

139 There were theoretical differences between both procedures. Firstly the pulse response model
140 was adjusted on a measured signal, acquired by placing the probes against each other. This
141 implied that the TOF of the signal within the instrument was taken into account by the model
142 and that the value obtained after cross-correlation was the TOF within the cheese alone. For
143 the response obtained with chirps, the TOF within the instrument was included in the
144 measurement and had to be subtracted. Secondly, the frequency response of the sensors

145 changed the shape of the chirps response and the maximum correlation (in the absence of noise)
146 which could be expected between the input signal and the response signal was less than one.

147 As both the output signals and the references were periodic functions, the result of the cross-
148 correlation (denoted *z*) were also periodic functions. The position of the signal was given by
149 the maximum of the correlation. The detection is quite straightforward when the signal is well
150 defined, such as in Fig. 4, but became less and less so when the signal decreases, particularly
151 for the echoes (Fig. 5). The maximum of the envelope curve *e* was then detected. This
152 envelope curve was evaluated using the Hilbert transform (Preumont, 1990) by computing :

$$e(t)=\left[z^2(t)+\hat{z}^2(t)\right]^{1/2} \tag{3}$$

153 where *z* is the result of the cross-correlation, $\hat{z}$ its Hilbert transform. The detailed results of
154 these treatments are shown in Fig. 4 for the pulse in transmission and in Fig. 5 for the pulse in
155 echo (control cheese), while the envelope curve is given in Fig. 6 for the chirp response in
156 transmission. The value of the maximum correlation indicates the quality of the pulse signal
157 and its position gave the TOF. The relative amplitude a_r of the signal *x* to the model *y* is given
158 by the ratio of the corresponding standard deviations :

$$a_r=\frac{s_x}{s_y} \tag{4}$$

159 For the pulse, this relative amplitude is close to one for the signal acquired by placing probes
160 against each other (on which the model was adjusted) and decreases when the sample is
161 inserted between the probes. For the chirps, it is always lesser than one (the reference being the
162 excitation).

163 2.4.2. Decomposition of the output signals into wavelets

164 The output signal was decomposed into nine levels of wavelets with the highest level
165 containing the “mother-function coefficients” and the other levels containing the remaining
166 wavelet coefficients (Press *et al.*, 1992). The lower the level, the shorter were the wavelets. In

each level, the position of the coefficients was related to the position of the signal. The number of coefficients increased by a factor of 2 as the level lowered. The wavelets were calculated using the Daubechies sets with 2, 4 and 12 coefficients. It was found that the transforms of the pulse gave signals in mainly two of the lowest levels, the second and the third. After re-sampling the third level, the coefficients were added to the second one (result in Fig. 7) and used directly for the detection of the pulses.

This method was only applied to the pulse responses.

2.5. Signal evaluation

For both methods, the results of the detection was a peak and noise as observed in Figs 4 to 8, or several peaks in the presence of an internal discontinuity (Fig. 9). In order to characterise the different signals and methods, the noise was characterised by its standard deviation and the peaks by the maximum values. The ratio of the maximum to the standard deviation gave the quality of each algorithm. Here, this will be called the signal to noise ratio (noted SNR).

With a poor quality signal, such as the echo or in case of big objects or bubbles, the amplitude of the maximum linked to the signal could be as low as the maxima resulting from the noise. It seemed then relevant to determine when a signal was significant, i.e. when the maximum was unlikely to be a random noise effect. The probability density function $g(z_n)$ of the maximum of a data set, comprising n items, sampled from a population with a normal probability density function $f(z)$ is given by (Dagnelie, 1998; the kind of probability function is, of course, an assumption) :

$$g(z_n) = n\left[\int_{-\infty}^{z_n} f(z)\,dz\right]^{n-1} f(z) \qquad (5)$$

The probability of observing a value as high as the maximum of the sample is given by the distribution function $g(z_n)$. Given a confidence level α and the different sample sizes, the minimum value for the maximum of the signal to noise ratio could be computed. It varied from

190 3.3 to 4.4 for $\alpha = 0.05$ to 0.001.

191 ***2.6. Defect detection***

192 The easiest way to detect a foreign object is to detect its echo. However for a cheese without
193 any internal object there is always the echo of the opposite face and the time of flight has to be
194 taken into account. Preliminary studies showed that the characteristics of the cheese such as
195 the sound speed or its dimensions varied from cheese to cheese and also with time for each
196 cheese. For this reason, taking into account only the echo was not enough.

197 For the cheese containing no inclusion or no major cavities, the transmitted signal arrived at the
198 receiver after a time of flight t_1. The reflected part of the signal returned to the emitter at time
199 t_2, such that $t_2 = 2 \times t_1$. The internal defects (holes or inclusions) will cause some modification
200 of the wave path, some attenuation of the transmitted signal and some reflection.

201 The first attempt to detect these defects was performed by characterising the signals (the echo
202 and the transmitted one) by global parameters. The times of flight and the maximum
203 amplitudes were first considered. As the echo signal showed several maxima in the presence of
204 a defect, the standard deviation quantifying the dispersion of the whole signal and the Pearson's
205 first coefficient b_1 quantifying the degree of symmetry, were supposed to be affected and were
206 also computed. Preliminary tests showed that the presence of an object had indeed an influence
207 on these parameters but the temperature of the cheese or its maturity also had a major
208 influence, in such a way that these parameters could not be used to detect a foreign object.

209 Another way to characterise the results was to detect the peaks and retrieve one of the
210 reflection patterns presented in Fig. 10. The first scheme corresponded to a cheese without
211 internal object (in our experiment, the control cheese), with one signal arriving at time t_1 and
212 the echo arriving at time t_2 (Fig. 10-a). In the second case, encountered in presence of an
213 internal defect, a part of the wave was reflected while another part was transmitted (Fig. 10-b).
214 There was a first echo at t_3 while the one at t_2 was still observed. In transmission, there was a

pulse arriving at t_1 (though with a lower amplitude than in the previous case) and possibly a second one at t_4. A third case was observed in presence of a defect and corresponded to most of the first wave going through the defect, reflected on the other side of the cheese and then again reflected by the defect, back to the transmission transducer side, arriving at t_5 (Fig. 10-c). These different schemes were observed with different samples, depending on the configuration of defects. The times t_1 to t_5 are related to the thickness of the cheese l and to the distance of the defect from the origin l_1 (provided that the signal is emitted at $t_0 = 0$) :

$$
\begin{aligned}
t_1 &= \frac{l}{v} \\
t_2 &= \frac{2 \times l}{v} \\
t_3 &= \frac{2 \times l_1}{v} \\
t_4 &= \frac{2 \times l_1 + l}{v} \\
t_5 &= \frac{l + 2 \times (l - l_1)}{v}
\end{aligned}
\qquad (4)
$$

where v is the speed sound.

The transmitted signal was investigated for local peaks showing a maximum correlation of at least 0.02 and having a half-height duration of more than 2.5 µs. Since the echo signal was noisier, the threshold to detect a maximum was set to the 95th percentile of the signal itself whilst maintaining the same half-height duration (25 µsec).

In order for a cheese to be declared fit for purpose, it had to have peaks at t_1 and t_2, with $t_2 > 1.9 * t_1$ and no peaks at t_3, t_4 and t_5. If any one condition failed, the sample was rejected.

2.7. Signal acquisition

When using correlation, the signal was sampled at 10 MHz, triggered by the emission, and thousand points were acquired (thus over a duration of 10^{-4} s). When using wavelets, the signal was sampled at 8 MHz and composed of 1174 points. In each case, the first 150 points were

234 neglected in order to eliminate the emission. For the transmitted signal, the maximum range
235 was 20 mV, while for the echo signals, the maximum range was 4 V for the pulses and 12 V for
236 the chirps. This was a compromise between the saturation of the signal by the excitation pulse
237 and the possibility of measuring the feeble echoes properly.

238 **3. Results**

239 Figure 3 shows the parametric model fitted by cross-correlation on a signal acquired by placing
240 probes against each other (validation signal). The correlation was 0.96. In this case the peak
241 cross-correlation was at zero (not shown in the figure). It can be seen that the model was well
242 fitted to the signal for the main part, up to 6 µs. After this time, the "tail" of the signal was no
243 more in phase with the earliest part. This phenomenon was supposed to come from the internal
244 reflection of the signal in the sensors and was at the origin of "secondary" peaks, close to the
245 main peak (Figs 4-c and 6). Including this part in a more complicated model would only add
246 secondary peaks which would complicate the detection of the main ones caused by small
247 internal defects. This problem was overcome by selecting the local maxima which had a mid-
248 height width above a given threshold (2.5 µs).

249 Figure 4 shows three diagrams, the first one being a transmitted pulse signal (Fig. 4-a) and the
250 reference fitted by cross-correlation, with its amplitude adjusted using Eq. 4 (the ratio was of
251 0.21); the second one is the response of the cross-correlation (Fig. 4-b) and the last one
252 represents the diagram envelope (Fig. 4-c). The main peak of the cross-correlation
253 corresponded to the beginning of the signal and gave the time of flight. Two secondary peaks
254 are visible. Figure 5 shows the same diagrams for an echo. Several differences were noted.
255 First, the noise was much higher, because the sensing ranges were different as explained in
256 section 2.7. The echo signal was also smaller than the transmitted one, the amplitude ratio was
257 0.046. Then there was a scale bias between the signal and the reference, because the standard
258 deviation of the signal s_x in Eq. 4 had a component linked to the signal and a component linked

to the noise. This was not noticeable when the noise was feeble compared to the signal, as shown in Fig. 4-a, but it can become important otherwise. As long as the noise was constant, the bias remained the same. This did not affect the time of flight evaluation.

The result of the detection of the chirps on the transmitted signal (Fig. 6) was very similar to the detection of the pulse. The correlation was slightly higher and one secondary peak was clearly visible. The wavelet transform (Fig. 7) presented sharper and multiple peaks.

Figs 8 and 9 show the SNR for a particular sample and for the different methods. Table 1 gives the mean and standard deviation (between samples) for the maximum SNR for each of the three methods, in relation to temperature and for the transmitted signal, the echo of the opposite face of the cheese and the echo due to the object. Comparing the transmitted signals and the echo (Figs 8 and 9), it can be observed that the SNR of the former was up to 30 times that of the latter. The amplitudes of the signals in Figs 4 and 5 indicates that the transmitted signal was around ten times higher than the echo, while the noise in the echo was much more important due to the different sensing ranges, as noted earlier. The enhancement of the echo could be obtained by using different probes for emission and echo.

The result of the t test comparing the means of the different methods (Table 1) are given in Table 2. For the transmission signal (Tables 1 and 2 and Fig. 8), all methods gave a much higher SNR than the significant threshold (more than 200 times the threshold - section 2.5) and no differences between signal or methods were significant. All the methods were thus convenient to detect the transmitted signal. On the other hand, for the echo (Tables 1 and 2 and Fig. 9) all the differences were at least highly significant and the responses could be classified starting with the best one as follows : as chirp and cross-correlation, pulse and cross-correlation, pulse and wavelets. However, all the three methods were far above the significant threshold (about ten times the threshold) which means that the detection of the echo is easily feasible. For the echo of the objects (Tables 1 and 2 and Fig. 9), 'pulse and cross-correlation', 'chirp and cross-correlation' presented no significant difference while 'pulse and wavelets' was

lower (highly significantly different from the other two methods). The mean signal to noise ratios of the object's echo were above the threshold, but not far away. For pulse and correlation method for example, the mean SNR was 8 while the standard deviation was of 4.8 and the upper limit of the confidence interval of the maxima was of 3.3 (for $\alpha = 0.05$). The second condition which was requested for a peak to be accepted as a detected signal, a mid-height peak width of 2.5 µs or more was necessary to sort out noise and signal. The instance of erroneously detected object echo given in Table 3 were in accordance with the signal to noise ratio. The methods based on correlation gave better results than the detection based on the wavelet transform, but could not be discriminated between the type of signal (pulse or chirps). When considering the on-line applicability of the method, the correct recognition rate at cellar temperature (14°C) was 90%, while considering the correlation based methods (Table 3).

There was no significant statistical influence of the temperature on the signal to noise ratio when examining the whole set of data (Table 1).

The residual standard deviation, characterising the variability of the SNR between the repetitions of the measurements on one sample (Table 4), was low compared to the standard deviation between the samples (Table 1). This former standard deviation was also smaller than the differences observed between measurements made several minutes apart, for which the temperature varied only by one degree Celsius. This suggests that the placement of the probe had an important effect on the measure. The force with which the probe was applied on the cheese was controlled and could thus not be a reasonable source of variation. To overcome the dependence of measurement sensitivity with the way the probes are placed, further studies can use non contact probes, such as the one presented by Cho and Irudayaraj (2003) for Cheddar cheese. Moreover, this last technique would present a major advantage since it would facilitate on-line defect control.

4. Conclusions

There is a demand in cheese-making industries for foreign body detection that could provide means to enhance process control and quality assurance. Within this scope, a method to detect foreign bodies in semi-soft cheeses of Trappist type by using ultrasounds was researched. The main problems encountered were the high attenuation of the signal due to the cheese texture (and especially the crust) and the acoustic impedance of the foreign body that was close to the cheese. For these reasons and because of the small size of the foreign body, the signal to noise ratio of the echo of the object was low. Furthermore, the raw signal was dependant on the temperature and on the maturity of the cheese, which justified the use of the time of flight of both the transmitted signal and the echo to detect the foreign body.

Input signals such as pulse and chirp were found to be efficient to detect foreign body. The signal analysis was based on the cross-correlation between a model and the output of the transmitted signal and the echo. Both signals gave similar results, showing a correct recognition rate of around 90%. The correlation with the model gave better results than the detection based on the wavelet decomposition. No significant effect of the temperature was observed.

Due to the robustness of the signal treatment, this technique can potentially be used in non-contact ultrasonic systems.

Acknowledgements

This research was funded by the Ministry of Agriculture, Walloon Region, project D31-1127.

References

Benedito, J., Carcel, J.A., Sanjuan N., Mullet, A., 2000, Use of ultrasound to assess Cheddar cheese characteristics. *Ultrasonics*, 38, 727-730.

Coupland, J. N., 2004. Low intensity ultrasound. *Food Research International*, 37, 537-543.

333 Cho, B.-K., Irudayaraj, J. M. K., 2003. Foreign Object and Internal Disorder Detection in Food
334 Materials Using Noncontact Ultrasound Imaging. Food Engineering and Physical
335 Properties, 68 (3), 967-974.

336 Dagnelie, P., 1998. *Statistiques théoriques et appliquées – Tome 1 Statistique descriptive et*
337 *bases de l'inférence statistique*. Deboeck Université, Bruxelles. pp, 508. ISBN
338 2-8041-2770-2.

339 Gunasekaran, S., Ak, M. M. , 2003. *Cheese Rheology and Texture*. CRC Press LLC, Florida.
340 pp 437. ISBN 1-58716-021-8.

341 Graves, M., Smith, A., Bruce, B., 1998. Approaches to foreign body detection in foods.
342 *Trends in Food Science & Technology*, 9, 21-27.

343 Hæggström, E., Luukkala, M., 2001. Ultrasound detection and identification of foreign bodies
344 in food products. *Food Control*, 12, 37-45.

345 Lee, H. O., Luan H., Daut, D. G., 1992. *Use of an ultrasonic technique to evaluate the*
346 *rheological properties of cheese and dough*. Journal of Food Engineering, 16, 127-150.

347 McClement D. J., 1995. Advances in the application of ultrasound in food analysis and
348 processing. *Trends in Food Science & Technology*, 6, 293-299.

349 McFarlane N.J.B., Bull, C.R., Tillett, R.D., Speller, R.D., Royle, G.J., 2001. Time Constraints
350 on Glass Detection in Food Materials using Compton Scattered X-rays. *J. agric. Engng.*
351 *Res.*, 79 (4), 407-418.

352 Povey, M. J. W., Mason T.J., 1998. *Ultrasound in Food Processing*. Blackie Academic &
353 Professional. London. pp. 282. ISBN 0-7514-0429-2.

354 Preumont, A., 1990. *Vibrations aléatoires et analyse spectrale*. Presses polytechniques
355 universitaires romandes. Lausanne. pp. 343. ISBN 2-88074-183-1.

356 Press W. H., Teukolsky S.A., Vetterling W.T., Flannery B.P., 1992. *Numerical Recipes in C –*

357 *Art of Scientific Computing – Second edition.* Cambridge University Press. Cambridge.
358 pp. 994. ISBN 0 521 43108 5.

359 Zhao, B., Basir, O.A., Mittal, G.S., 2007. Hybrid of multi-signal processing methods for
360 detection of small objects in containers filled with beverages using ultrasound. *LWT –*
361 *Food Science and Technology*, 40, 655-660.

362 Table 1 : Signal to noise ratios (SNR) for the different methods, at different temperatures, for
363 transmission, echo and echo due to the object. The mean values are reported with standard
364 deviation between cheeses stated within brackets.

Signal	t° (°C)	Pulse & cross-correlation	Pulse & Wavelets	Chirp
transmitted	4	641 (305)	410 (171)	945 (757)
	10	508 (303)	476 (179)	522 (315)
	14	693 (83)	540 (246)	487 (286)
	17	663 (394)	484 (272)	431(197)
echo	4	41.5 (21.6)	13.1 (2.9)	65 (22)
	10	69.2 (33.2)	32.8 (18.6)	94 (37)
	14	107 (15.8)	59.0 (13.1)	110 (37)
	17	33.7 (15.4)	15.6 (7.4)	56 (32)
echo in presence of the foreign body	4	13.2 (8.1)	5.0 (2,6)	11.2 (10.0)
	10	12.8 (8.4)	7.3 (7.4)	13.8 (6.8)
	14	8.0 (4.8)	4.9 (2.1)	7.1 (7.6)
	17	4.35 (2.3)	3.1 (0.6)	8.2 (8.9)

365

366

Table 2 : t tests for the equality of the mean signal to noise ratios given in Table 1.

Comparison	Probability
Transmission P(SNR_{PM}=SNR_{PW})	0.069
Transmission P(SNR_{PM}=SNR_{C})	0.603
Transmission P(SNR_{C}= SNR_{PW})	0.279
Echo P(SNR_{PM}=SNR_{PW})	0.000
Echo P(SNR_{PM}=SNR_{C})	0.003
Echo P(SNR_{C}= SNR_{PW})	0.000
Echo object P(SNR_{PM}=SNR_{PW})	0.001
Echo object P(SNR_{PM}=SNR_{C})	0.948
Echo object P(SNR_{C}= SNR_{PW})	0.000

Table 3 : Error rate in object detection for the different methods. Data are given for the entire temperature range and for the cellar temperature (13 -14 °C).

	Pulse & cross-correlation	Pulse & Wavelets	Chirp
4 – 17 °C	10.3%	34.1%	12.1%
13 – 14 °C	10.0%	45.0%	8.8%

374 Table 4 : Mean residual standard deviation (mean standard deviation between the repetition of

375 each sample), for samples at the cellar temperature (13 -14 °C).

Signal	Pulse & cross-correlation	Pulse & Wavelets	Chirp
transmitted	34.2	33.3	18.2
echo	9.6	1.9	3.9
echo with foreign body	1.8	0.8	3.9

376

377

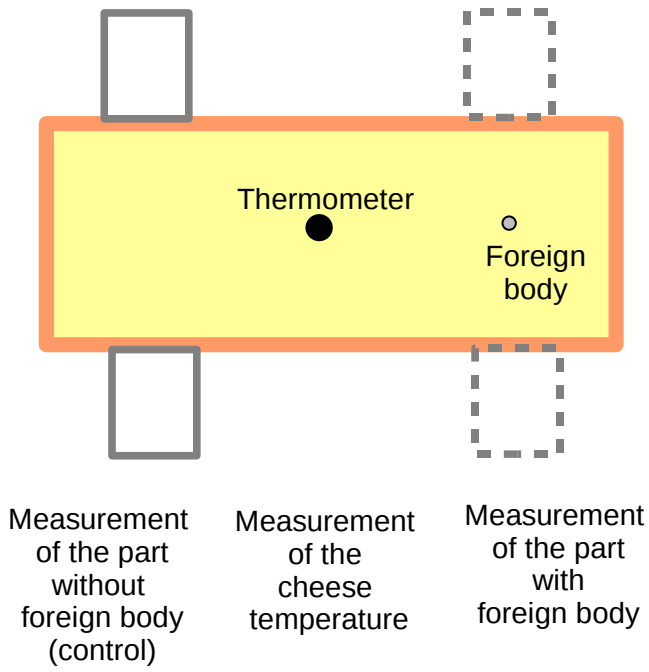

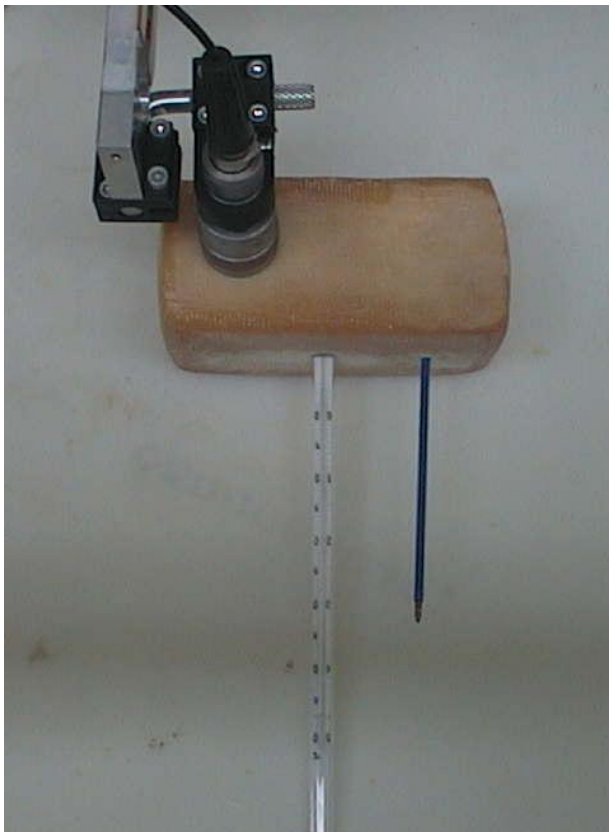

378

379 Figure 1 : Acquisition device

380

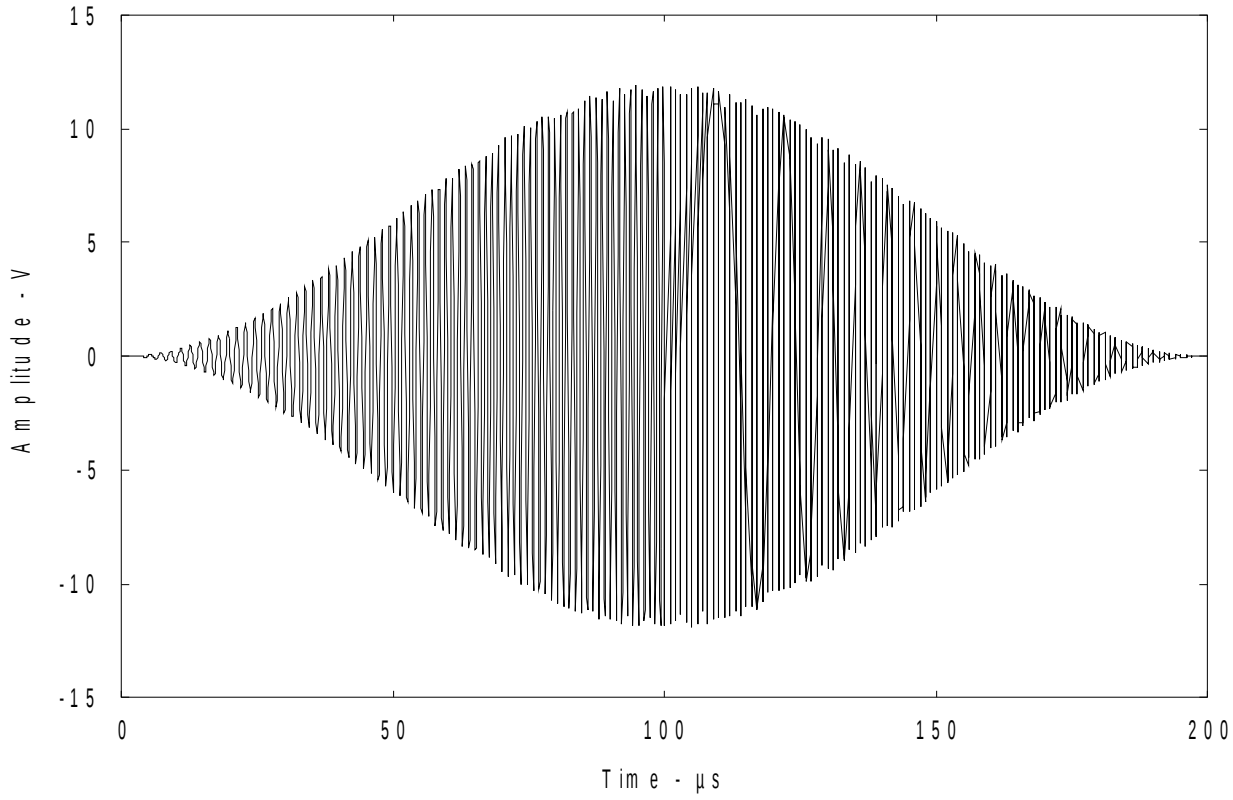

381

382 Figure 2 : The chirp signal

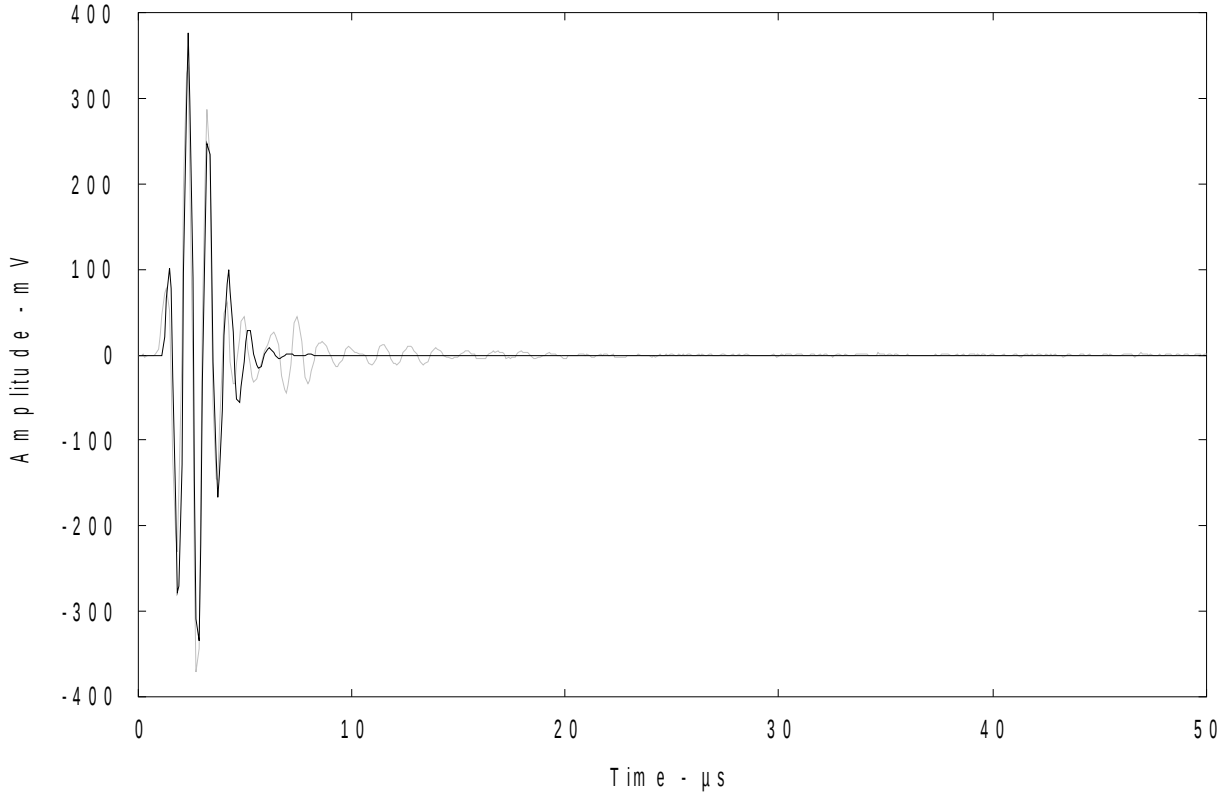

383

384 Figure 3 : Typical response to a pulse input [probes placed against each other (light grey curve)

385 and the parametric model fitted to it (thin black curve)]

a

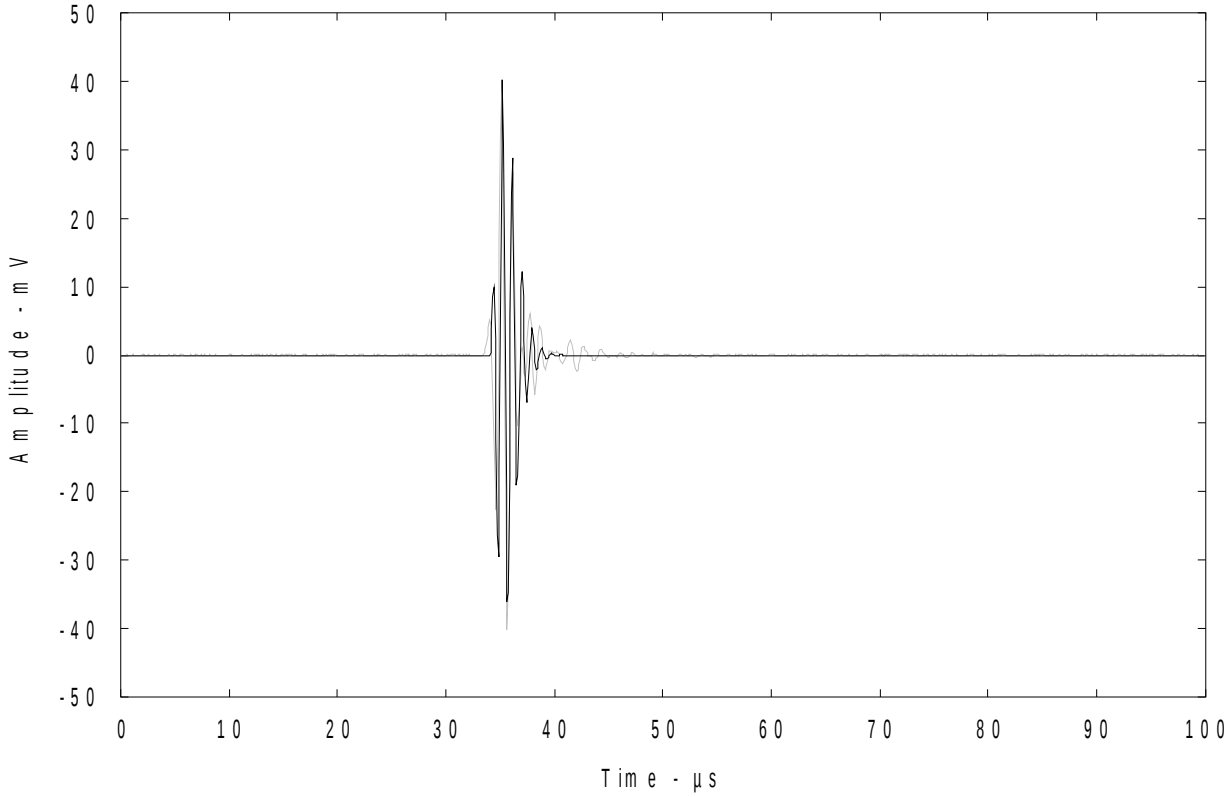
50
40
30
20
10
0
-10
-20
-30
-40
-50
Amplitude - mV
0
10
20
30
40
50
60
70
80
90
100
Time - µs

b

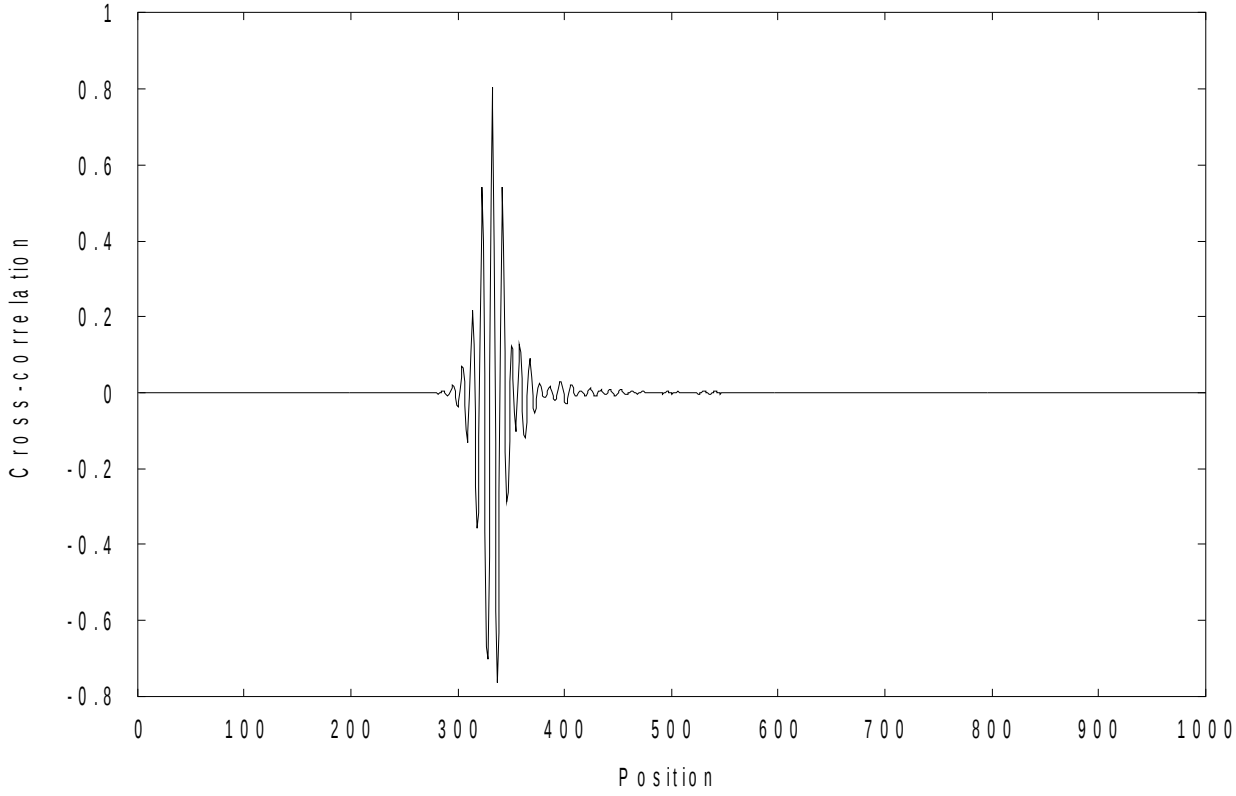
1
0.8
0.6
0.4
0.2
0
-0.2
-0.4
-0.6
-0.8
Cross-correlation
0
100
200
300
400
500
600
700
800
900
1000
Position

c

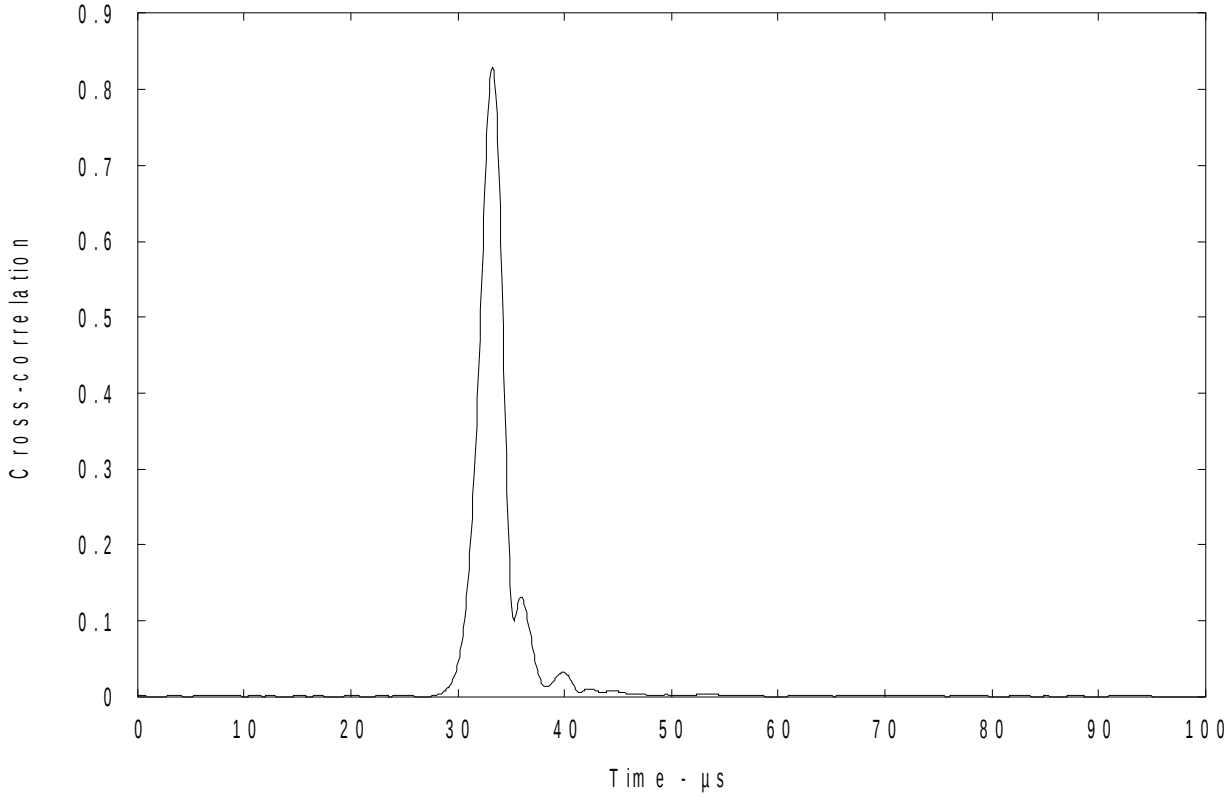

386 Figure 4 : Pulse response, transmission through cheese without any foreign object (control). a :
387 row signal (light grey curve) and the model of the signal positioned at the highest cross-
388 correlation (thin black curve); b : Cross-correlation and c : Hilbert transforms

389

a

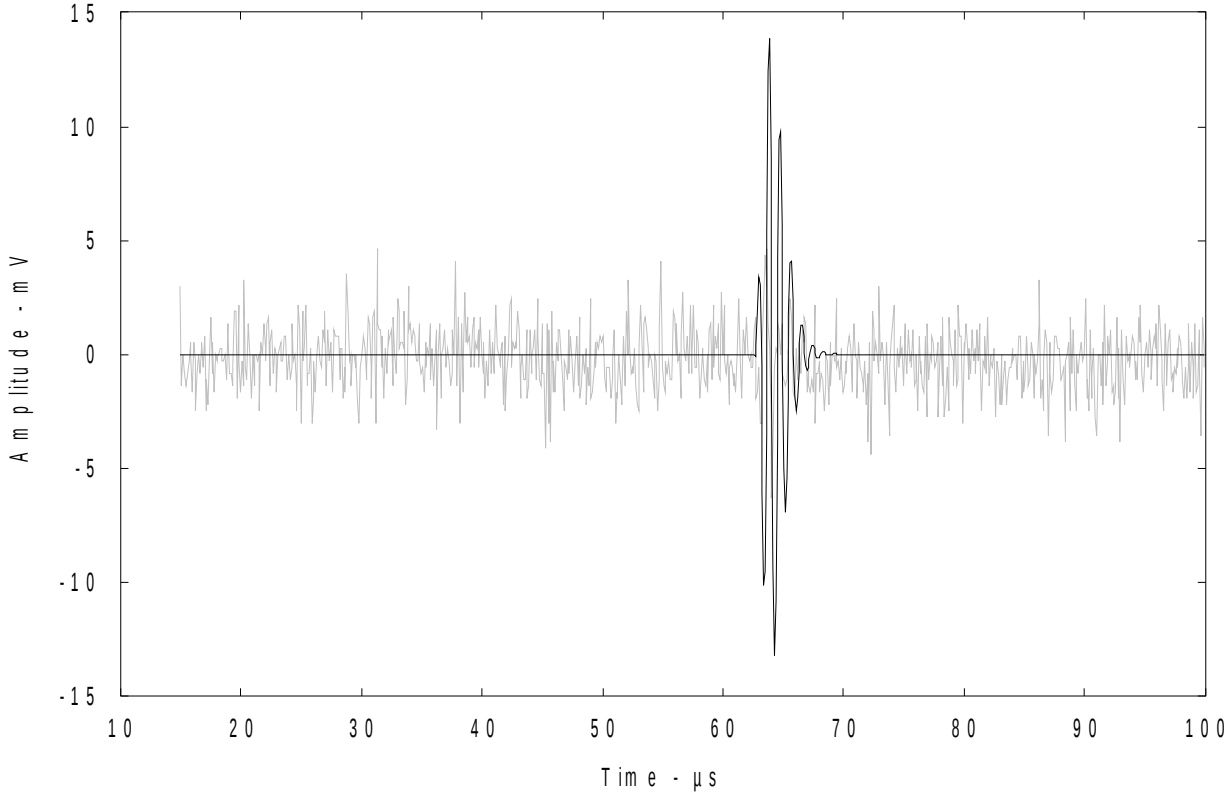
15
10
5
0
-5
-10
-15
Amplitude - mV
10
20
30
40
50
60
70
80
90
100
Time - µs

b

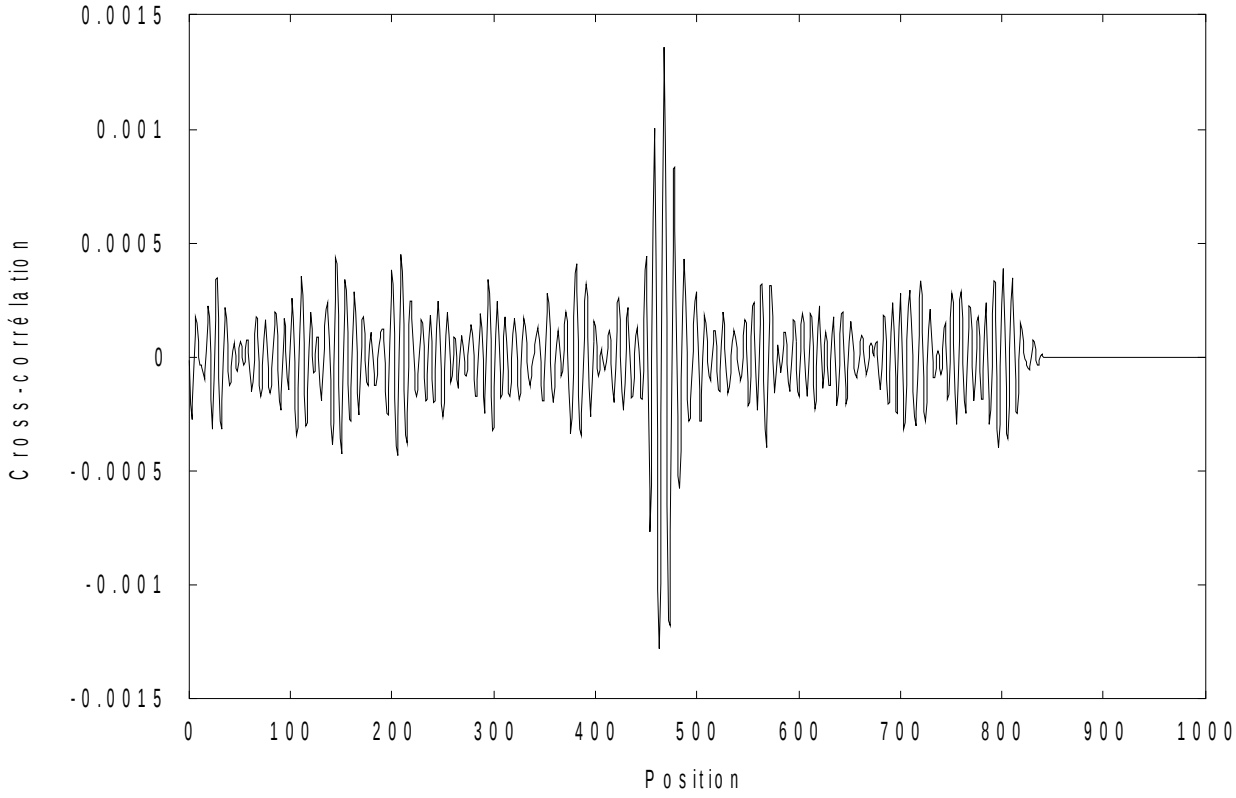
0.0015
0.001
0.0005
0
-0.0005
-0.001
-0.0015
Cross-corrélation
0
100
200
300
400
500
600
700
800
900
1000
Position

c

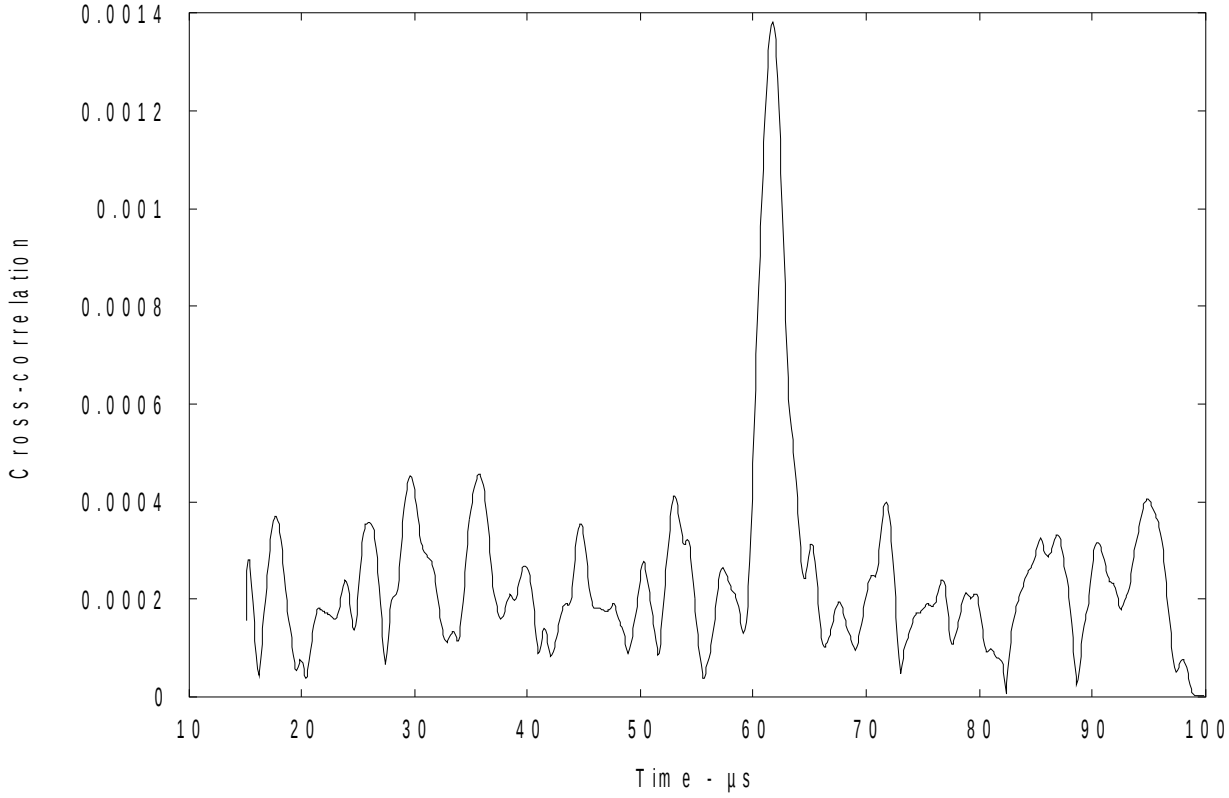

390 Figure 5 : Echo (pulse response) acquired by the emitter transducer. a : raw signal (light grey
391 curve) and the model of the signal positioned at the highest cross-correlation (thin black
392 curve); b : the cross-correlation of the signal and the model; c : the envelop of the cross-
393 correlation

394

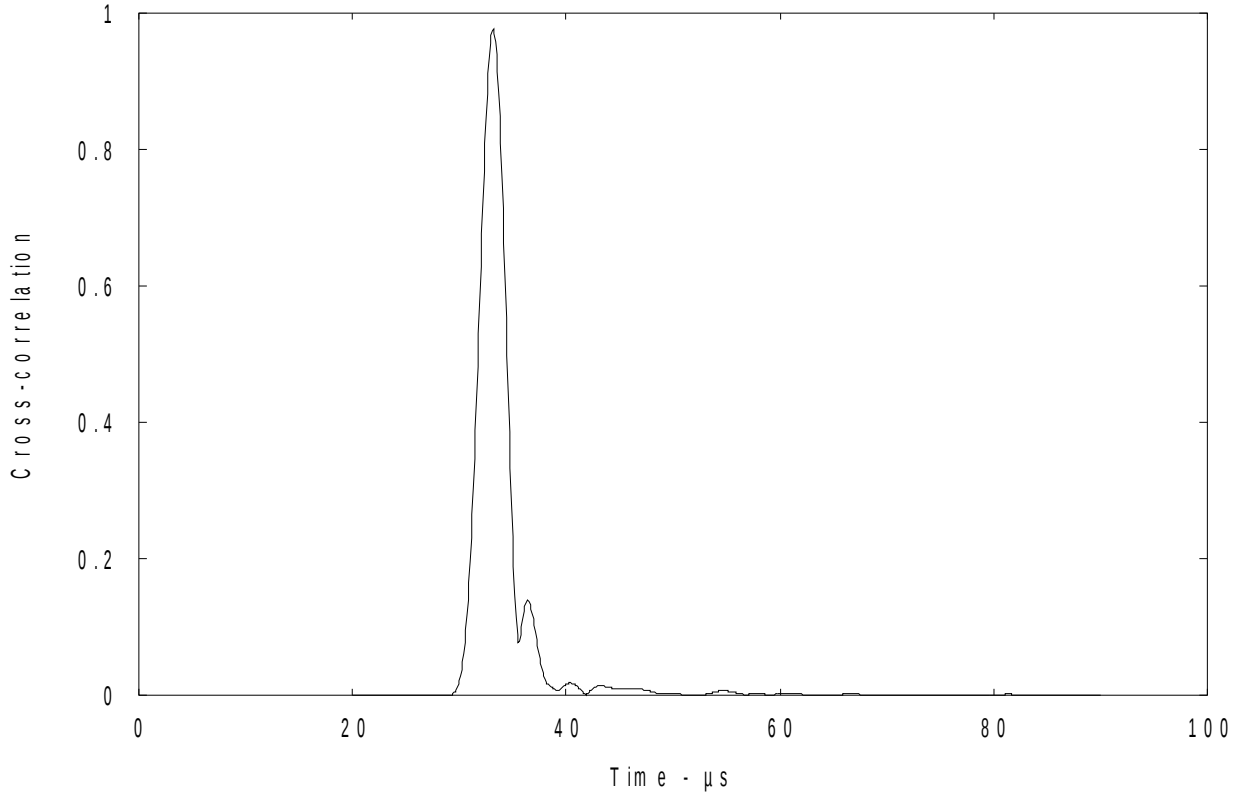

395

396 Figure 6 : Result of the Hilbert transforms for the cross-correlation of the response to a chirps

397 signal

398

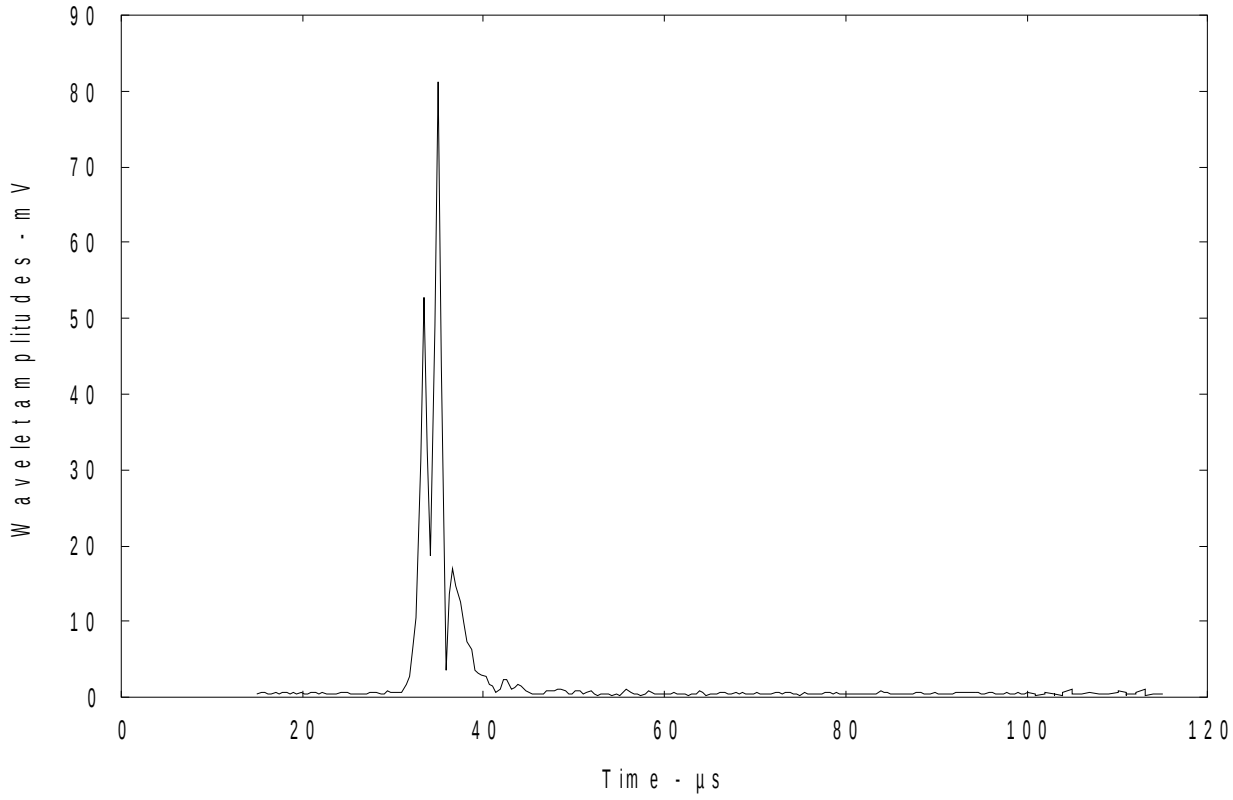

399

400 Figure 7 : Sum of the third and second level wavelet decomposition of the signal transmitted

401 through cheese

402

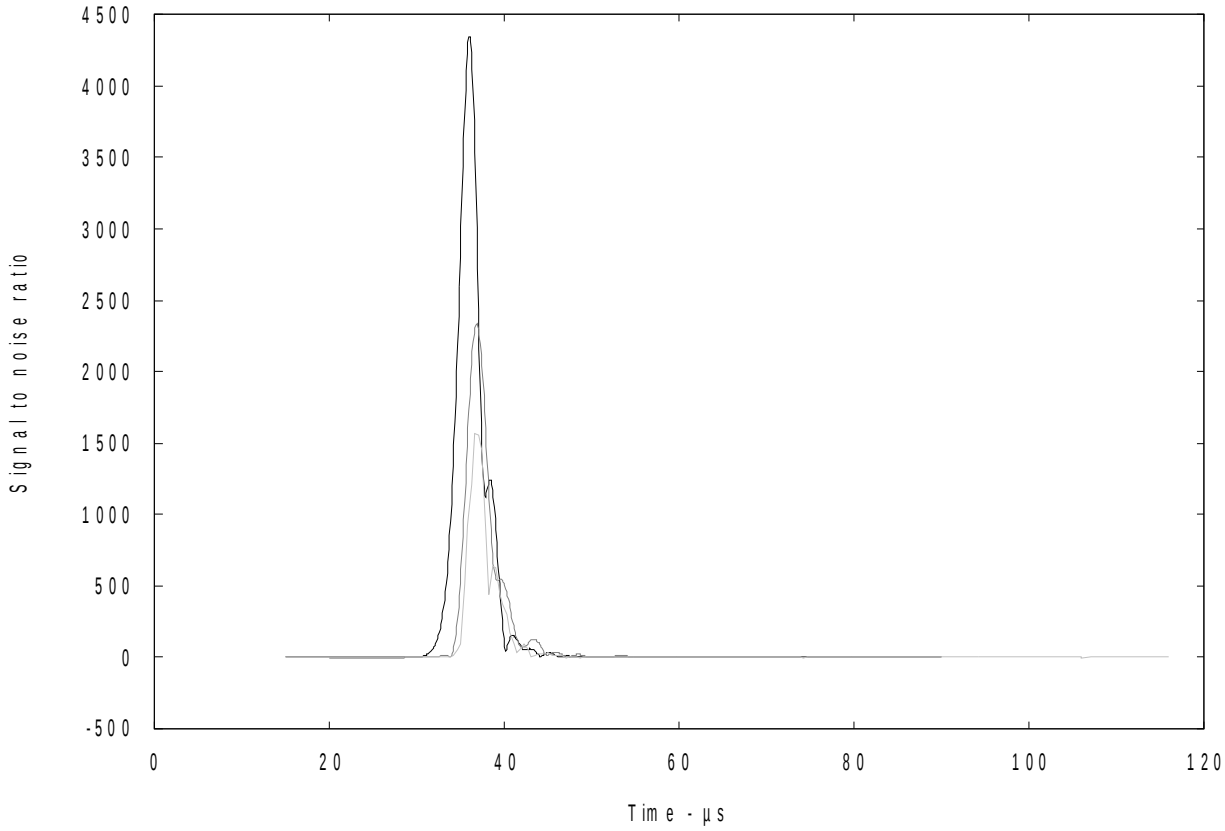

403

404 Figure 8 : Signal to noise ratio for the transmitted signal from cheese containing the foreign
405 body. Black thin curve : pulse and cross-correlation; dark grey medium curve : chirps and
406 cross-correlation; ligth grey thick curve, pulse and wavelets

407

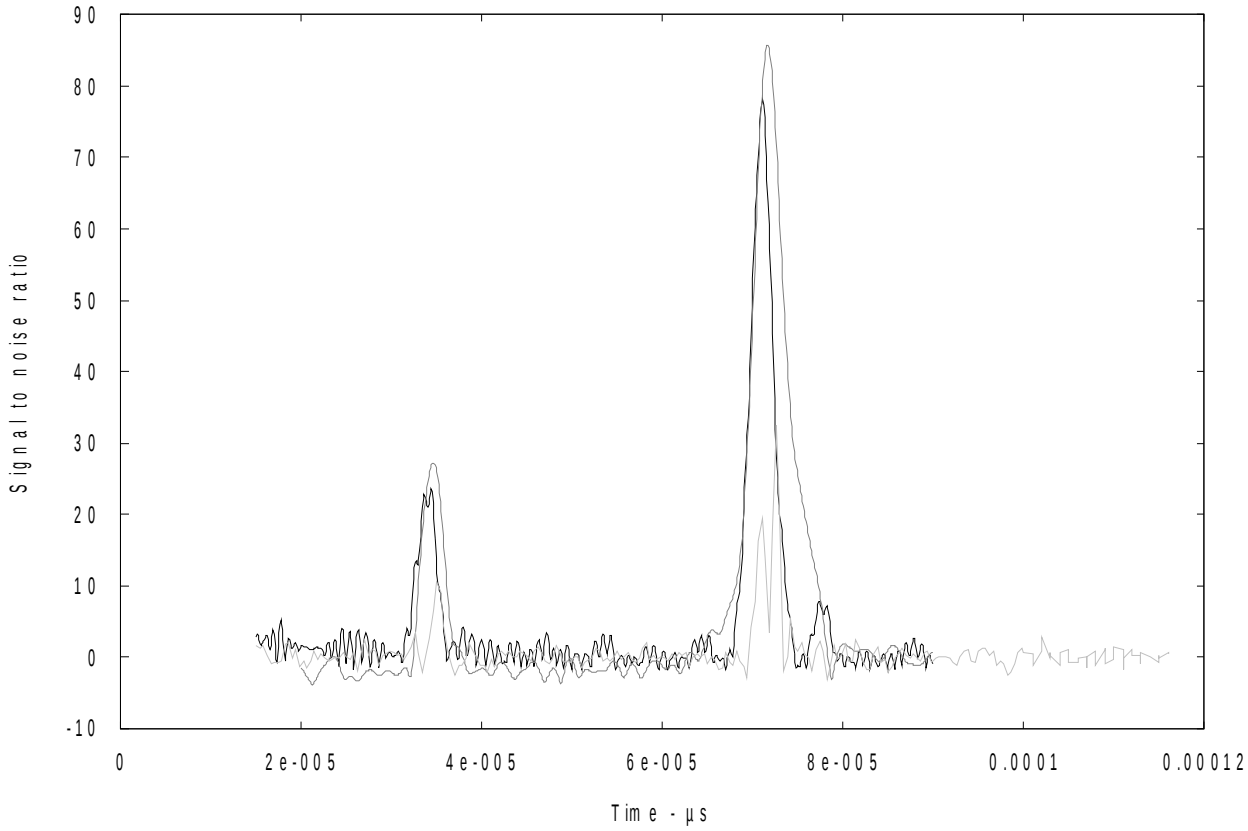

408

409 Figure 9 : Signal to noise ratio, for the echo from the cheese cheese containing the foreign
410 body. Black thin curve : pulse and cross-correlation; dark grey medium curve : chirps and
411 cross-correlation; light grey thick curve, pulse and wavelets

412

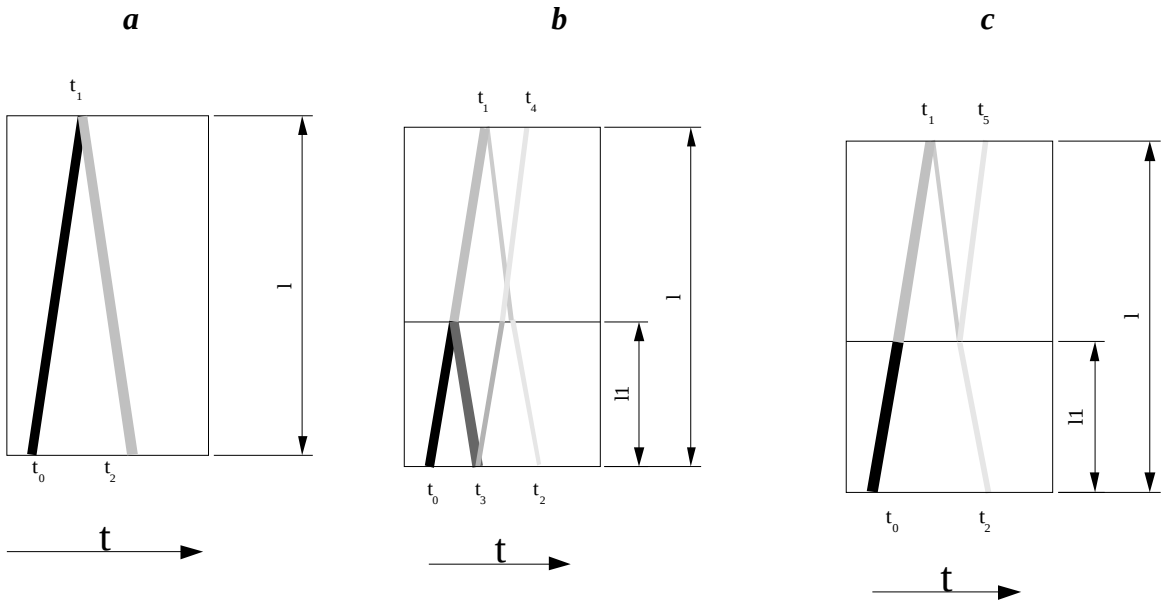

413 Figure 10 : Different possible ultrasound wave reflection patterns. a : without an internal object,

414 b and c : with an internal object